Renewable Energy 181 (2022) 833–842

Contents lists available at ScienceDirect

Renewable Energy

journal homepage: www.elsevier.com/locate/renene

Techno-economic selection and initial evaluation of supercritical CO_2 cycles for particle technology-based concentrating solar power plants

Lukas Heller [a, *], Stefan Glos [b], Reiner Buck [a]

[a] German Aerospace Center (DLR), Institute of Solar Research, Stuttgart, Germany
[b] Siemens Energy, Mülheim an der Ruhr, Germany

ARTICLE INFO

Article history:
Received 15 June 2021
Received in revised form
19 August 2021
Accepted 1 September 2021
Available online 15 September 2021

Keywords:
Supercritical CO_2
CSP
Particle technology
Techno-economic optimization

ABSTRACT

In this study, the techno-economic performance of supercritical carbon dioxide (sCO_2) power cycles in concentrating solar power plants based on particle technology is assessed. A simplified levelized cost of electricity calculation was used to investigate the effect of cycle parameters, compare cycle layouts and allow for comparing optimized sCO_2 power blocks with steam technology. Results showed that simple cycle layouts with fewer components and lower cycle parameters lead to the lowest energy cost. This is caused by (a) fewer components, (b) lower primary heat exchanger, turbine as well as recuperator cost if the turbine inlet temperatures is limited and (c) a lower cost of the thermal storage system if the sCO_2 temperature increase in the primary heat exchanger is large. Nevertheless, even the most economical sCO_2 variants generate electricity at a 10 % higher cost than a steam reference system and a significantly lower efficiency. These results held true when changes were made to cost models. Finally, it was shown that the cost of main sCO_2 equipment would have to be reduced by 30 %–50 % to reach cost parity with steam systems. These findings will need to be confirmed with more detailed off-design simulations and optimized solar field components.

1. Introduction

It is generally agreed on, that future electricity generation has to come predominantly from renewable energy sources. Compared with the other technologies that allow for a large increase in deployment, i.e. wind power and photovoltaics, Concentrating Solar Power (CSP) can be equipped with a cost-effective, multi-hour thermal energy storage. It is, therefore, not a fluctuating source to an electric grid but can offer dispatchable power on demand.

In order to make CSP plants more cost competitive with alternative electricity generation technologies, for example fluctuating renewables plus electric batteries, the levelized cost of electricity (LCOE) generated by them needs to be lowered. Typically, the power block is the subsystem with the lowest efficiency in a CSP plant. An increase in its efficiency would decrease the size of all solar equipment (collector field, receivers, towers and thermal energy storage), which accounts for the majority of a solar tower plant's direct costs [1]. Furthermore, the power block itself accounts for approximately 30 % of these costs. Improvements in its efficiency or cost can, therefore, have a large impact on CSP plants' technical and economic performance.

For many years, power blocks employing supercritical carbon dioxide (sCO_2) as the working fluid have been suggested to reach both, higher thermal efficiencies and lower costs, compared with state of the art steam cycles [2]. These potential advantages make the technology attractive for utilization in next generation CSP plants and several studies have been conducted on predicting the performance of such systems [e.g., 3,4].

Most of these studies feature comparisons of different cycle layouts, mainly simple recuperated cycles, recompression cycles, partial cooling cycles and even more complex ones. Glos et al. [5], for example, compared the thermal efficiency of three CO_2 cycles with that of a steam reference system. They found a performance improvement only for a high-performance recompression cycle with reheat and intercooling, not for a simple recuperated cycle, and only if highly effective recuperation is assumed. Ho et al. [6] calculated the investment cost of CSP plants featuring several cycles with identical power rating. A simple recuperated and a recompression cycle had very comparable total cost and thermal efficiency.

Crespi et al. [7] as well as Neises and Turchi [8] modeled CSP

* Corresponding author.
E-mail address: Lukas_Heller@gmx.de (L. Heller).

https://doi.org/10.1016/j.renene.2021.09.007
0960-1481/

Nomenclature

Variables

C	cost (USD)
$LCOE$	levelized cost of electricity (USD/(kW$_e$ h))
TTD	$= T_{\text{hot side,out}} - T_{\text{cold side,in}}$, terminal temperature difference (K)
UA	heat exchanger conductance-area product (W/K)
η	efficiency (%)
Δp	relative/absolute pressure drop (%)/(Pa)

Subscripts

a	annual
dp	design point
e	electrical
m	mechanical
t	thermal

Abbreviations

BoP	balance of plant
CSP	concentrating solar power
DNI	direct normal irradiance
EPC	engineering, procurement and construction
HP	high-pressure
IC	intercooling
LCOE	levelized cost of electricity
LP	low-pressure
PB	power block
PHX	primary heat exchanger
RH	reheat
sCO_2	supercritical carbon dioxide
TES	thermal energy storage
TIT	turbine inlet temperature

systems with molten salt as the heat transfer medium, which induces strict limitations on temperatures and high cost penalties on small temperature differences between hot and cold storage tanks. With these effects considered, they each identified partial cooling cycles as the most economical sCO_2 cycle layouts (excluding configurations that are not suitable for CSP applications). Furthermore, both studies found that a simple recuperated cycle had lower or the same LCOE as a recompression cycle (without reheat or intercooling).

Very few studies could be found that compare the techno-*economic* performance of power plants employing sCO_2 cycles with those employing state-of-the-art steam cycles and none of them included particle technology. Cheang et al. [9] compared a recompression and a partial cooling sCO_2 cycle with two steam cycles. As the modeled plants were designed using molten salt as the heat transfer fluid, the maximum sCO_2 temperature was limited to 580 °C and thermal efficiencies were found to be moderate. Cheang et al. concluded that existing steam cycle technology provided higher thermal efficiencies as well as lower installation costs and should therefore be pursued. Crespi et al. [7] derived ranges of LCOE for molten salt CSP plants with a steam and a sCO_2 recompression power block, respectively, using probabilistic cost models. Both configurations resulted in similar ranges, however, the identified spread of LCOE values was large.

Within the CARBOSOLA Project (funded by the German Ministry for Economic Affairs and Energy), Siemens Energy AG and the DLR intend to assess the economic performance of a next-generation sCO_2 CSP plant. In a previous publication by the authors of the present study [10], the techno-economic performance of sCO_2 cycles was compared based on cost models from literature. Under the chosen assumptions, systems based on molten salt as the heat transfer medium were found to lead to higher LCOE values than those based on particle technology.

Due to the lack of agreement in the literature on the optimal sCO_2 cycle for high-temperature CSP applications, a pre-assessment of a multitude of sCO_2 cycles and variants was conducted in the present study, using new cost and performance correlations for major sCO_2 cycle components. The components in the solar particle loop of the plant (namely, heliostat field, receiver, storage system and transport system), were modeled in a simplified manner to attain approximations for the annual electrical output of the plant and, therefore, be able to calculate estimated LCOE values. Based on this figure of merit, the most promising cycle layouts and parameters were chosen for further, more detailed studies. Furthermore, LCOE values of state-of-the-art steam cycles were calculated with the same model, allowing for a direct comparison of the two technologies in a particle technology-based plant.

2. Modeling and simulations

In this section the boundary conditions, details on the technical and economic modeling and the optimization approach are presented. Furthermore, reference systems featuring a steam power block are defined.

2.1. Location, solar field and particle loop modeling

The approximate capacity of the modeled power plant and its location are representative of a typical solar tower plant. The location has a high cumulative annual direct normal irradiation (DNI, see Table 1). In a typical year, the ambient temperature rarely exceeds 35 °C or drops below 0 °C at an annual mean of 19 °C.

The solar receiver is based on the CentRec® technology [11]. As this particle receiver is a cavity receiver with a small aperture opening, multiple towers are foreseen which feature individual heliostat fields. A schematic of such a particle loop is depicted in

Table 1
Plant location, boundary conditions and efficiency assumptions (a: annual; dp: design point).

Parameter	Value
Location	Postmasburg, RSA
DNI_a	2676 kWh/m^2/year
Design point	spring equinox, solar noon
DNI_{dp}	1000 W/m^2
$T_{\text{ambient,dp}}$	19 °C
Design PB capacity (semi-net)	115 MW$_e$
Solar multiple	2.5
TES capacity	12 h
$T_{\text{receiver,out}}$	900 °C
$T_{\text{cold tank}}$	286 °C to > 700 °C
Capacity per receiver,dp	96.2 MW$_t$
$\eta_{\text{collector,dp}}$	73.5 %
$\eta_{\text{collector,a}}$	52.7 %
$\eta_{\text{receiver,dp}}$	90.0 %
$\eta_{\text{receiver,a}}$	86.7 %
$\eta_{\text{dumping,a}}$	98.0 %
$\eta_{\text{plant,gross-to-net}}$	97.5 %
$\eta_{\text{PB,net,a}}$	$\eta_{\text{PB,net,dp}}$ x 99 %

Fig. 1. Important performance indicators of the receiver and heliostat field, which are based on initial simulations with the tool Visual HFLCAL [12] as well as of the complete plant are presented in Table 1. The receiver outlet temperature was fixed at 900 °C as this has been demonstrated for the technology [13], although higher values promise even better economic performance [14]. The cold tank temperature was calculated for each individual configurations depending on the sCO_2 inlet temperature to the particle heat exchanger and its terminal temperature difference.

For a given design point power block efficiency and particle temperature spread, the particle heat exchanger can be sized. The thermal energy storage (TES) system capacity and, therefore, particle inventory are designed to allow for 12 h of full-load PB operation. Under the design point conditions and efficiency estimates defined in Table 1, the heliostat fields, receivers, towers and particle transport systems are sized. Based on this information, the cost of the subsystems can be calculated with the cost models presented in Section 2.3. The annual electricity yield of the plant, $E_{e,\,a}$, is estimated in a simplified manner by multiplying the cumulative annual DNI, DNI_a, with the collector area, $A_{heliostats}$, and the annual average efficiencies of collector field, receiver, for dumping and of the power block:

$$E_{e,a} = DNI_a A_{heliostats} \times \eta_{collector,a}\eta_{receiver,a}\eta_{dumping,a}\eta_{PB,a}. \quad (1)$$

2.2. sCO_2 power cycle modeling

This study's focus is on the performance and economics of sCO_2 cycle power blocks in CSP plants. As a large number of cycle variants is to be compared in the initial stage, the annual energy yield calculation is simplified according to Equation (1). Therein, no hourly calculations are conducted for off-design ambient or load conditions of the power block. Instead, annual average values are used to approximate the electricity generation of any power cycle.

The only PB-related data that is adjusted for every variant in the energetic calculations is the design point net power block efficiency, $\eta_{PB,net,dp}$, which is calculated using the power plant simulation tool Ebsilon Professional v.14.03 by STEAG Energy Services GmbH, and, in consequence, the thermal input to the power block. Furthermore, parameters needed as input for the cost model of the sCO_2 power block (see Section 2.3) are derived from these simulations. Thermodynamic results were validated with data from the literature and very good agreement was found.

Based on a literature review, a total of ten process layouts were chosen to be modeled. They were simple recuperated cycles and recompression cycles with or without reheat (RH) or intercooling (IC) as well as partial cooling cycles with or without RH (see Table 2). The respective schematic of two cycles is shown in Fig. 2. The remaining cycle layouts can be derived by removing the highlighted components.

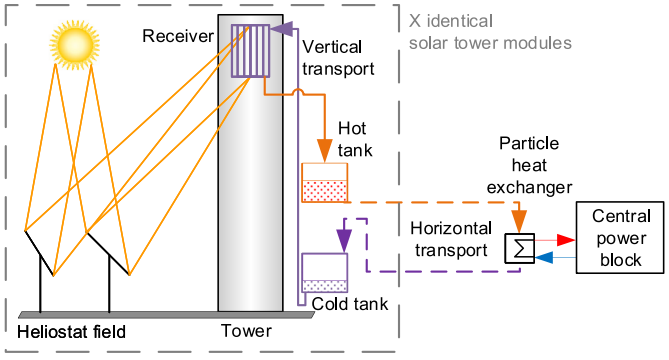

Fig. 1. Schematic of the solar particle loop.

2.3. Economic models

The methodology of the economic model is visualized in Fig. 3. The direct cost for power block equipment, C, is calculated according to mostly confidential models based on values of scaling factors (e.g., power rating or conductance-area product, UA), which are outputs of the Ebsilon models

$$C = (1 + d^{*}T_{reference} + e^{*}T_{reference}^2)(a + bx^c). \quad (2)$$

The specific values of the parameters a, b, c, d and e as well as the chosen scaling factor, x, are provided in Appendix A except for confidential information. The reference temperature, $T_{reference}$, for temperature-dependent cost adjustment is the maximum medium temperature in the component. For example, the equipment cost of a primary heat exchanger, PHX, is calculated as

$$C_{PHX} = \left(1 + d^{*}T_{Pa,\,in} + e^{*}T_{Pa,\,in}^2\right) {}^{*}3266.8\,\text{USD}\left(\frac{(UA)_{PHX}}{W_t/K}\right)^{0.66}, \quad (3)$$

with the values of d and e being confidential and $T_{Pa,in}$ representing the particle inlet temperature. It should be noted that no inflation adjustments were made due to the relatively narrow time window in which the cost figures were published (between the years 2018 and 2020).

Additionally, indirect costs of a technology provider including profits and contingencies are estimated as a cost adder of 83 % for all steam PBs and of 67 % for all sCO_2 PBs (the latter lower value is meant to account for lower predicted civil and installation costs due to more compact equipment)

$$C_{TP,PB} = C_{PB,equipment} + C_{sCO_2-PB,indirect} + C_{sCO_2-PB,profit} = \sum(C_{PB,equipment})\,167\,\%. \quad (4)$$

All items included as indirect costs are listed in Fig. 3.

The costs of all other subsystems of the power plant are calculated on the EPC (Engineering, Procurement and Construction) company level. The underlying correlations for these costs are also given in Table A5. To derive the total investment cost of the project, costs for EPC services and profit as well as owner services are added, which accounts for 31.4 % on top of EPC direct costs. The fixed charge rate, FCR, is calculated as 9.37 % for a project lifetime of 25 years and an annual interest rate of 8 %. Annual operation and

Table 2
Definition of sCO_2 cycle layouts (SR: Simple recuperated; Recomp: Recompression; PC: Partial cooling).

Name	Cycle type			RH	IC
	SR	Recomp	PC		
01	x				
02	x			x	
03	x				x
04	x			x	x
05		x			
06		x		x	
07		x			x
08		x		x	x
09			x	x	(x)
10			x		(x)

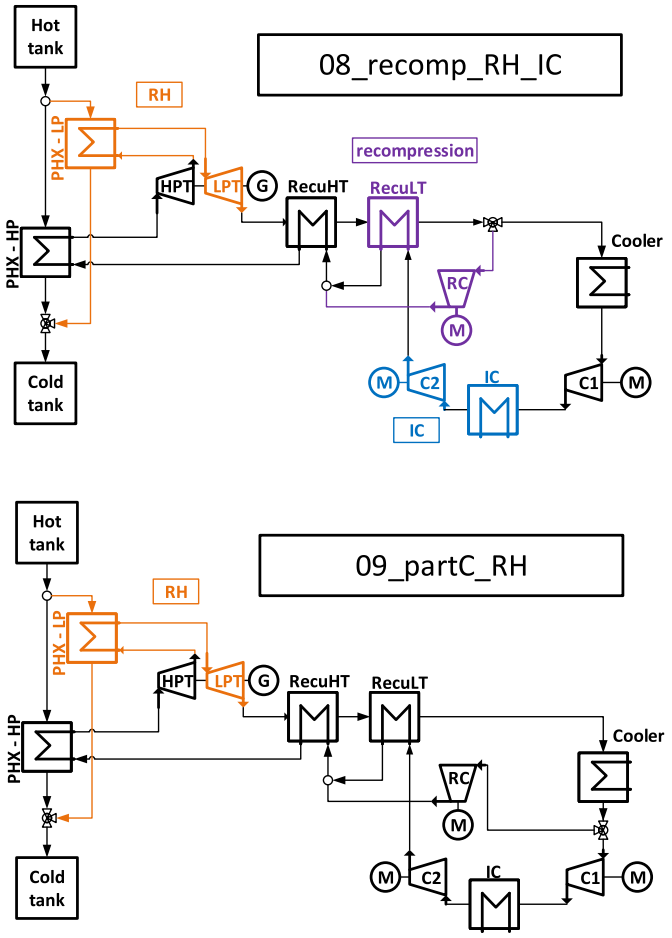

Fig. 2. Schematics of recompression cycle with RH and IC (top) and partial cooling cycle with RH (bottom); Components marked in color would be omitted for simpler cycle layouts (orange: RH, blue: IC, purple: recompression).

maintenance costs, $O\&M_a$, are further assumed to amount to 2 % of EPC direct costs. Overall, these assumptions for costs added to the EPC direct costs are more conservative than found in some other studies [e.g., 15] and would, therefore, result in less competitive LCOE values. However, as they are also used for the reference systems in this study and all plants are set to generate the same annual electric output, the comparisons remain valid.

2.4. Steam reference cycles

In order to compare the cost and performance results of sCO_2 PBs to commercially available technology, two steam cycles were modeled with the identical technological and economic assumptions, except for indirect costs (see Section 2.3) and, of course, PB equipment costs. The two reference cycles are a state-of-the-art subcritical RH steam cycle with a turbine inlet temperature (TIT) of 550 °C at a net PB efficiency of 42.7 % and a next-generation subcritical RH steam cycle with a TIT of 600 °C and a net PB efficiency of 43.6 %. Cost estimates for steam PB equipment were provided by Siemens Energy.

2.5. Simulation and optimization

Each of the ten sCO_2 cycle models was used to calculate net power block efficiencies under varying input parameters. A list of these parameters, as well as the ranges in which they were varied can be found in Table 3. Additionally, some relevant assumptions, which were either derived from component designs by Siemens Energy or estimated based on literature, are presented.

The simulation results were then used to size the remaining components of the CSP plant according to the methodology described in Section 2.1—i.e., to achieve the identical design-point electric power output for all configurations—and to calculate the cost of all equipment and subsystems as well as the respective LCOE values according to Fig. 3. For each configuration, the primary heat exchanger terminal temperature difference was optimized to minimize the LCOE.

3. Results and sensitivity analysis

In the following, results of the techno-economic pre-assessment are presented in several steps, with different focuses. Firstly, the overall LCOE optimization is presented, followed by a closer look at the optimum values of some varied parameters. Secondly, the calculated LCOE values and power block efficiencies are compared to those of the steam reference systems. Finally, the calculations are repeated with adjusted cost models to show the results' sensitivity to economic assumptions.

3.1. LCOE optima with original cost model

The net power block efficiency as well as the resulting LCOE value of all cycle variants are shown in Fig. 4. Several observations can be made from the plot:

1. There is a well defined pareto front marking the configuration with the lowest LCOE for any value of the power block efficiency.
2. The minimum LCOE for the sCO_2 cycles is located at a net PB efficiency of approximately 37 %, which is much lower than that of the steam reference systems.
3. The minimum LCOE of the sCO_2 cycles is considerably higher than that of either of the reference systems (as has been found by Cheang et al. [9] for molten salt plants with a much more restricted temperature range). As the commercially available steam cycle with a TIT of 550 °C is more economical than the 600 °C variant, the former is used as the reference for comparisons.
4. Very high efficiencies can be reached (greater than 49.0 %), as proposed in various sources in the literature [4,14,16]. This, however, leads to an approximately 30 % higher LCOE compared with the most economical sCO_2 configuration.
5. The lowest-LCOE configurations over the range of PB net efficiencies are predominantly based on cycle types "01", "05", "09" or "10". This is more obvious in Fig. 5, where only the pareto front per cycle layout is shown. This means that IC or RH are not economical under the used cost assumptions (which has also been found by Crespi [17] for molten salt plants), with the potential exception of partial cooling cycles. The sudden increases in LCOE seen in some of the pareto fronts in this plot are caused by discrete changes in TIT.
6. Absolute LCOE values for all variants, including steam systems, are higher than anticipated and calculated in recent studies [e.g., 15, 16]. However, these studies' economic assumptions, especially the fixed charge rate and the heliostat costs, are more optimistic than in the present study.

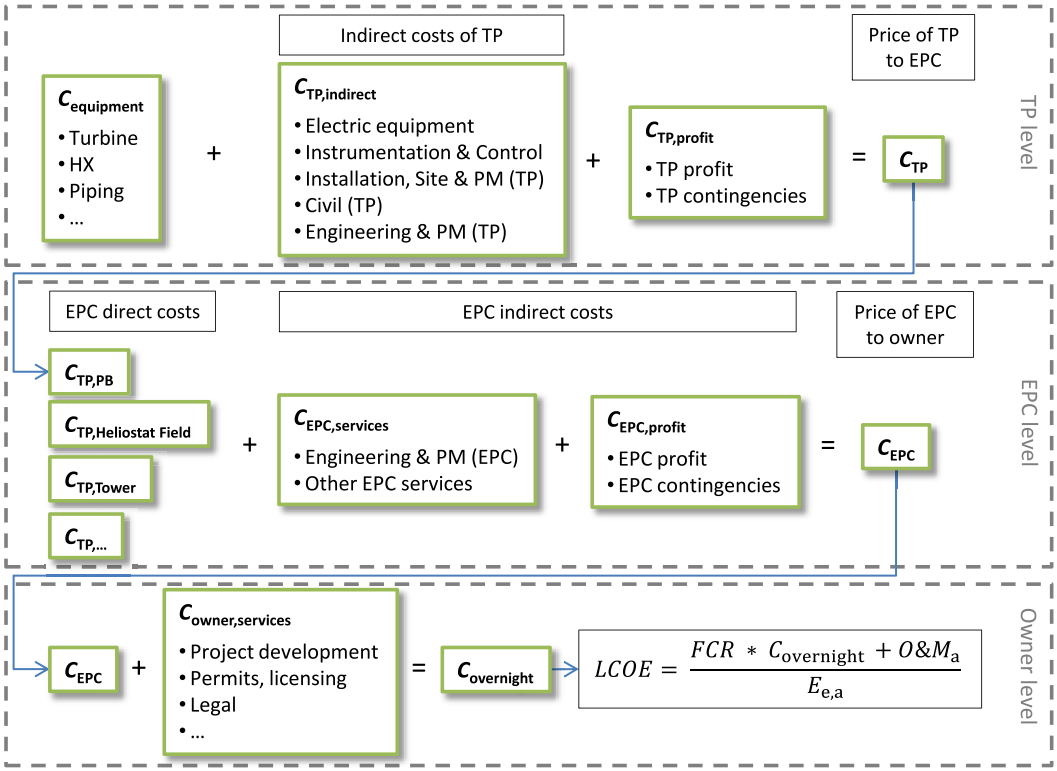

Fig. 3. Economic modeling methodology (TP: technology provider PM: project management).

Table 3
Assumptions and parameters of sCO_2 cycles (†: relative to design inlet pressure; §: pressures below 75 bar were only simulated for partial cooling cycles).

Parameter	Unit	Value
$\Delta p_{Recuperators}$ LP side	–	2 % †
$\Delta p_{Recuperators}$ HP side	–	3 % †
Δp_{PHX}	–	2 % †
$\Delta p_{Cooler/IC}$	–	0.6 % †
$\Delta p_{Cooler/IC,airside}$	mbar	5
$\eta_{Turbines, isentropic}$	–	91 %
$\eta_{Compressors, isentropic}$	–	87 %
$\eta_{Motors, e}$	–	97 %
$\eta_{Generator, e+m}$	–	98.7 %
$\eta_{PHX,t}$		99 %
Turbine inlet pressure	bar	260
TIT	°C	550 to 700
Compressor inlet pressure	bar	45 to 100 §
Recompression fraction	–	0.25 to 0.50
$(UA)_{Cooler/IC}$	MW/K	up to 18
Recuperator	K	5 to 80
TTD_{PHX}	K	5 to 295

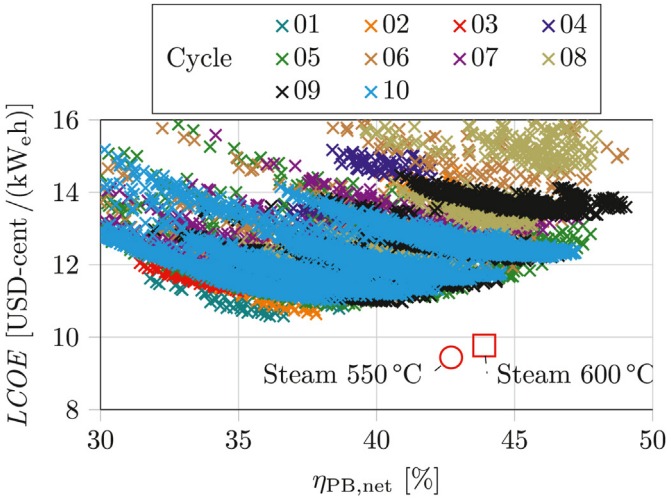

Fig. 4. Economic and energetic performance of all simulated variants (layout definition as per Table 2).

3.2. Optimum parameters

The low efficiencies of cost-optimized cycles is surprising given that sCO_2 power blocks are commonly proposed as a high-efficiency technology, at least in the field of CSP [8,14]. Interestingly, an optimization for LCOE benefits cycles with comparatively low TITs (see Fig. 6), which is contrary to findings in other studies, where either TITs greater than 700 °C are defined [7,16] or even found as an economic optimum [18]. This indicates that those components which are cost sensitive to the cycles' maximum temperature are dominating the overall cost. These are especially the PHXs and turbines through temperature-dependent cost multipliers (see Appendix A), as well as recuperators (due to a larger temperature increase and, thus, more heat being recuperated).

Furthermore, a higher TIT decreases the temperature difference at the hot side of the PHX, meaning that larger and more expensive heat exchangers are needed. This is visualized in Fig. 7, where the particle and sCO_2 temperature evolution in a PHX is shown for two, otherwise identical, configurations with different TITs. Additionally, the sCO_2 temperature at the inlet to the PHX, $T_{sCO_2,in}$, tends to be higher for configurations with a higher TIT or with a greater cycle efficiency, as the latter usually requires more effective recuperation. If the terminal temperature difference of the PHX, i.e. $TTD_{PHX} = T_{cold\ tank} - T_{sCO_2,in}$, is kept constant, this leads to an increase in the

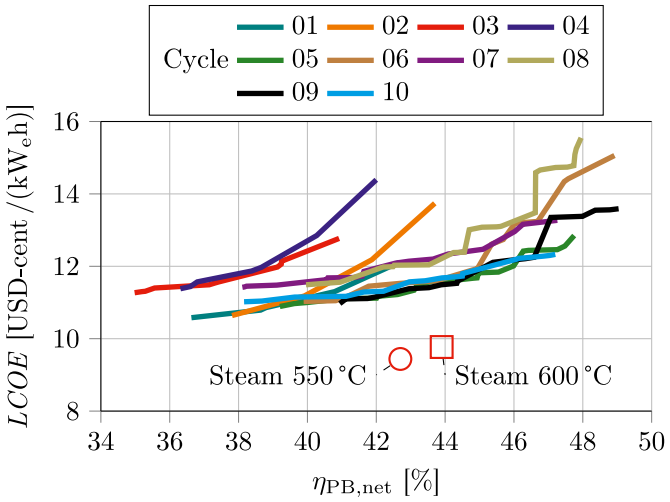

Fig. 5. Pareto fronts of all simulated cycle layouts (layout definition as per Table 2).

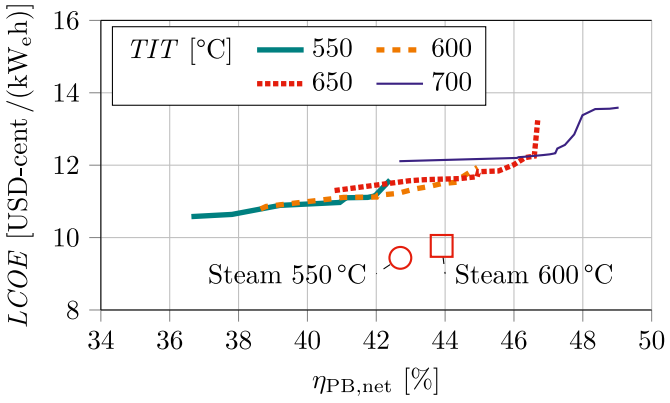

Fig. 6. Pareto fronts of all turbine inlet temperatures.

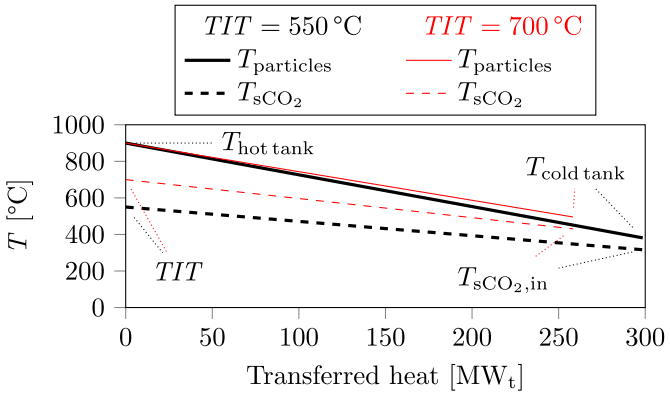

Fig. 7. Heat-temperature diagram of a PHX for two example configurations (*TIT* = 550 °C and *TIT* = 700 °C) indicating in- and outlet temperatures of particles and sCO_2.

cold tank temperature (also visible in Fig. 7) and, consequently, in the needed particle inventory as well as in the TES system's cost.

The cost-optimized balance between PHX and TES system is found by iterating the terminal temperature difference of the PHX. The plot in Fig. 8 depicts the sCO_2 inlet temperatures to the PHXs (low-pressure, LP, and high-pressure, HP) as well as the cold tank

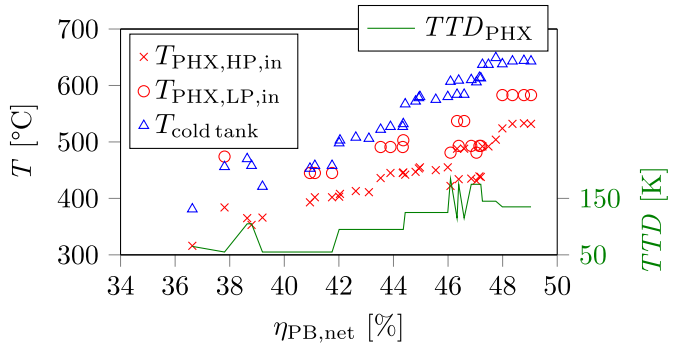

Fig. 8. PHX sCO_2 inlet and cold tank temperatures for pareto optimal configurations with a variation in the terminal temperature difference of the PHX.

temperature for those configurations that define the pareto front, i.e., those with the lowest LCOE. When moving towards high-efficiency configurations, there is an obvious trend towards higher PHX inlet temperatures, which is partially caused by higher TITs and partially by more effective recuperation in recompression or partial cooling cycles. The cold tank temperature increases at an even higher rate, as the LCOE-optimized PHX terminal temperature difference (green line) increases from approximately 50 K for low-efficiency configurations up to approximately 150 K. The temperature spread in the TES system varies, therefore, between more than 500 K and a minimum of 250 K, with associated cost implications. An additional increase in structural and insulation costs for the cold tank due to higher operating temperatures has been neglected, which would further benefit low-efficiency configurations.

The range of values of further input parameters that resulted in pareto optima are the following: For non-partial cooling cycles, the influence of changes in compressor inlet pressure are small and a value of 75 bar is almost always optimal. Recuperators and cooling heat exchangers (coolers plus ICs) in the optimum configurations are large at optimum parameters of 10 MW/K to 40 MW/K (5 K–15 K TTD) and 9 MW/K to 15 MW/K, respectively. The optimum recompression fraction ranges mostly from 35 % to 40 % except for partial cooling cycles, where it reached up to 46 %. These ranges are in agreement with other studies on optimum cycle parameters for the chosen boundary conditions, for example by Dyreby et al. [2].

3.3. Component costs

The LCOE of sCO_2 systems was found to be considerably higher than that of steam systems (see Section 3.1). In order to identify the main drivers, the direct equipment cost of sCO_2 components, power block indirect cost and relevant subsystem costs are shown in Fig. 9(top). The three configurations being compared are the steam reference case (blue bars), a sCO_2 system with a similar power block efficiency to that of the reference (orange bars) and, lastly, the sCO_2 system with the lowest LCOE (green bars). The main cycle parameters of these configurations are presented in Table 4. Comparing the cost contributions of all three systems, the following can be observed:

- There is a significant difference in PHX cost between the sCO_2 case with comparable efficiency to the steam cycle and the other configurations. This is mainly caused by the increased TIT (to 600 °C) and the use of RH, which necessitates an additional PHX component.

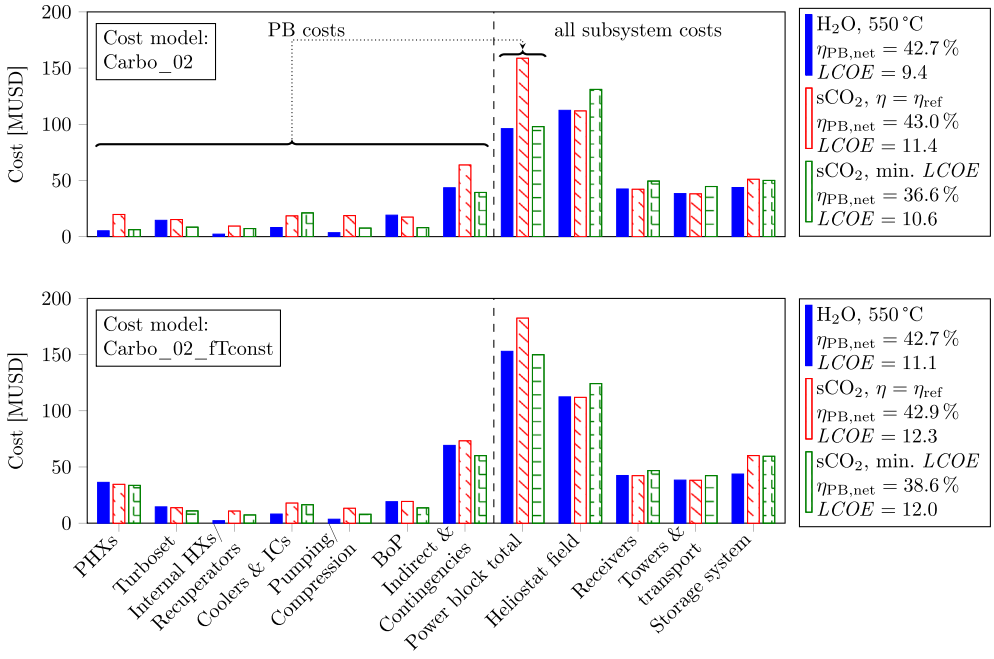

Fig. 9. Comparison of PB component costs and all subsystem costs for developed cost model (top) and adjusted PHX cost models (bottom); *LCOE* in [USD-cent/(kW$_e$h)].

Table 4
Parameters of configurations shown in Fig. 9(top) (†: heat rate-weighted mean of HP and LP flow).

Parameter	Unit	H_2O	sCO_2	
			η_{ref}	*LCOE*
Cycle layout			09	01
TIT	°C	550	600	550
Recompression fraction	–		0.40	
$(UA)_{Cooler+IC}$	MW/K		10.1	14.0
$(UA)_{Recuperators}$	MW/K		13.1	10.0
$T_{PHX,fluid,in}$	°C	258 †	458 †	316
$T_{cold\ tank}$	°C	400	522	381

- Recuperators and coolers in sCO_2 cycles induce much higher costs than internal heat exchangers and condensers in steam cycles. The same is true for compressors, especially in complex cycles featuring several ones, compared with feed water pumps.
- Costs for sCO_2 turbosets (i.e., turbines plus generator) and balance of plant (BoP) only have lower costs than the reference if the TIT is low and no RH is employed.
- The total cost of the sCO_2 PB far exceeds that of the reference system unless a much lower cycle efficiency is accepted. In that case, the cost for other subsystems increases as they need to provide more energy to the PB.
- The higher sCO_2 inlet temperatures of high-efficiency cycles lead to an increase in cold tank temperature (see Fig. 8). This leads to larger particle inventories and, therefore, higher TES system cost. This effect is even more pronounced for recompression cycles (not shown).

3.4. Sensitivity

During the definition of equipment cost models, it was observed that there is a large uncertainty associated especially with the costs of particle-sCO_2 PHXs. Due to the lack of any commercial or even demonstrator-size implementations to date, cost models for the component vary widely. Particularly challenging is the correct consideration of the effect of operating temperatures on used materials and, therefore, cost. So far, this has only been investigated in research projects.

The PHX cost model, which was employed in all previously presented results of this study, is of the form

$$C_{PHX} = \frac{f_{T,PHX}}{f_{700\ °C}}\ 3266.8\ \text{USD}\left(\frac{(UA)_{PHX}}{W_t/K}\right)^{0.66}. \quad (5)$$

Therein, $f_{T,PHX}$ is a confidential multiplication factor depending on the TIT and $f_{700\ °C}$ represents the value of the factor at a TIT equal to 700 °C. The rest of this correlations was derived from literature [14] and converted to be conductance-area product-specific by assuming an overall heat transfer coefficient equal to 300 W/m^2 K.

The previously defined cost model results in a strong temperature-dependency of the PHX cost, which leads to potentially unrealistically low costs at low TITs. For a lack of better data available, the sensitivity of overall plant economics on the factor $f_{T,PHX}/f_{700\ °C}$ was assessed by re-evaluating all concepts with the temperature-dependency removed. This is obviously a very conservative assumptions for the lowest TITs. The results derived by use of this cost model ("Carbo_02_fTconst") are shown in Fig. 9(bottom). Naturally, the PHX costs for all variants are higher compared with the previous cost model. Although the absolute costs are, thus, also higher for all sCO_2 cycles, the cost of the reference system increase as well and the difference in minimum LCOE between the fluids is smaller. However, the general trend is unchanged.

Furthermore, it was determined by how much the costs of major sCO_2 equipment would have to be lowered in order to reach cost parity with the steam reference cycle. To achieve this, a lower limit for cooler and IC costs (according to Siemens Energy) is assumed, and direct cost of turboset, recuperators, compressors as well as the indirect cost adder are multiplied by a factor (<1) for every configuration until parity is reached. Using the original cost model ("Carbo_02") as the base, it was found that those costs would have

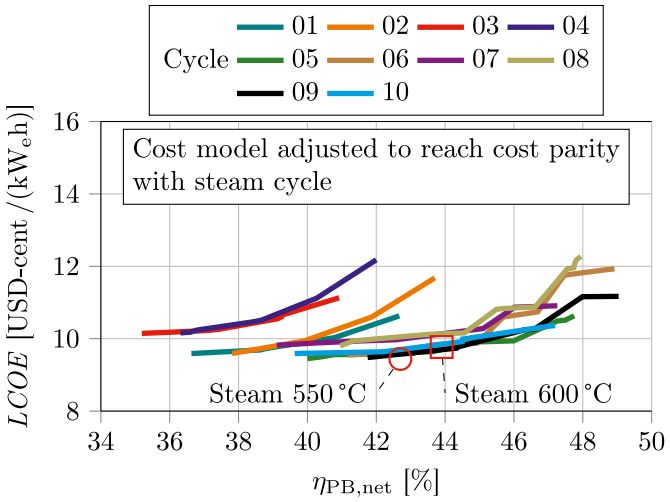

Fig. 10. Pareto fronts of all simulated cycle layouts for assumed cost parity with the reference system (layout definition as per Table 2).

to be halved to reach cost parity. If cost model "Carbo_02_fTconst" (s.a.) is employed, which penalizes the cost of steam cycles comparatively more than those of sCO_2 cycles, the same analysis showed that those costs would have to be lowered by at least 30 %.

3.5. Cycle selection

The selection of a small number of the most promising sCO_2 cycles is one of the key deliverables of this study. The pareto fronts per cycle shown in Fig. 6 imply that if the lowest LCOE is the sole figure of merit, a configuration of Layout 01 should be chosen, while if a higher cycle efficiency in sought after, Layout 05 or one the partial cooling layouts could be beneficial. As cost models have a large influence on the results of the presented analysis, the same comparison is shown in Fig. 10 for the previously introduced cost model with 50 % lower costs for certain equipment (see Section 3.4). It can be deduced that the same cycle layouts would be chosen from an economic point of view. While under these extremely optimistic cost assumptions Layout 01 does not have a clear cost benefit over Layout 05 and the partial cooling cycles any more, it still remains competitive.

3.6. Discussion of deviation from other studies' results

There are various reasons for the apparent disagreement of our findings with the common perception of sCO_2 power cycles as a highly promising economical technology.

Firstly, not many studies could be found in which the cost of sCO_2 power blocks is calculated in a similar level of detail as in the presented work. Here, cost assumptions are based on cost figures from an internationally active supplier of power plants and power cycle components. When subsystem-level costs are estimated for the PB, these are commonly significantly lower than those found in this study [e.g. 14]. Often, even cost targets are used [16].

Secondly, compared with studies in which PB costs are calculated, differences in the component cost models compared with the ones used here have been observed. Indirect costs are an important cost driver and there are differences in the way cost items are allocated either as direct or indirect costs. Compared to other studies [e.g. 7,18], our indirect costs are significantly higher, even though optimistic assumptions have been applied.

Thirdly, literature data for steam systems' investment cost or LCOE values are sometimes used as reference values for calculated values of sCO_2 PBs. An analogous modeling of a reference system with comparable input data and boundary conditions can limit the effect that uncertainties, especially of economic and financial models, have on the comparison.

3.7. Next steps

As a next step, several areas of the models should be refined. The presented study is based on design point evaluations. Deeper investigations should consider part-load operation conditions of the power cycle. An hourly energy yield model that takes into consideration power block efficiencies under non-nominal cooling conditions will be implemented in a follow-up study. However, as sCO_2 cycles are expected to be penalized more by changing ambient temperatures than steam cycles, these changes are not expected to tilt the scale in their favor.

A further detailed optimization of thermal storage and solar field configuration would help to slightly improve technical configurations and to find global LCOE minima for sCO_2 and the reference systems.

Lastly, many of the cost models for sCO_2 equipment, indirect power block cost and particle subsystems have a large uncertainty due to their low technology readiness level. While we are confident that our models represent the best state of knowledge, extensive component development and testing, which is currently under way in numerous sCO_2- and particle technology-related pre-commercial projects, will increase accuracy in the future.

4. Conclusions

A simplified techno-economic model was developed to estimate the LCOE of next-generation CSP power plants utilizing an sCO_2 power block. A multi-tower particle receiver system based on the CentRec® concept with a receiver outlet temperature of 900 °C and a 12 h thermal storage is used. Ten different power block layouts (derivatives of simple recuperated, recompression and partial cooling cycles) were modeled and their key parameters varied to find economic optima based on developed cost models for the main power block components and indirect cost. The LCOE optimum was, somewhat surprisingly, found for simple recuperated cycles without reheat or intercooling with a net power block efficiency of less than 37 %, much lower than the one of a state-of-the-art reference system with a steam cycle power block (42.7 %). As a general finding, simple recuperated and recompression cycles resulted in lower costs if reheat and intercooling was omitted.

Furthermore, a comparison with the steam reference system showed that the sCO_2 systems' LCOE is at least 10 % higher. As some of the cost models, especially the one of the particle-to-sCO_2 heat exchanger, have a high uncertainty, the economic comparison was repeated with variations to the original model. However, the general trend appeared mostly unchanged. It was found that the costs of sCO_2 power block main components as well as indirect cost adders would have to be lowered by 30 %–50 % to reach cost parity with steam systems.

Several refinements to the simulations are proposed, namely off-design modeling, solar field and thermal energy storage optimization as well as more accurate component cost models, which will hopefully be available in the future.

CRediT authorship contribution statement

Lukas Heller: Conceptualization, Methodology, Software, Writing – original draft. **Stefan Glos:** Methodology, Investigation, Writing – review & editing. **Reiner Buck:** Conceptualization,

Methodology, Writing – review & editing.

Declaration of competing interest

The authors declare that they have no known competing financial interests or personal relationships that could have appeared to influence the work reported in this paper.

Acknowledgements

The authors would like to thank the German Federal Ministry for Economic Affairs and Energy for the financial support of the project CARBOSOLA (reference number: 03 EE5001C). Furthermore, thanks are due to Mr. Tobias Hirsch for his valuable feedback on the manuscript.

Appendix A Component cost models

Table A5
Cost models (*: confidential data; if no source is mentioned, the correlation was created within the CARBOSOLA Project; assumed exchange rate: 1 EUR = 1.10 USD; $\dot{V}_{in}$: volumetric flow rate at inlet; H_{tower}: height of receiver center above tower base; $\dot{Q}_{Rec,t}$: receiver thermal rating; Q_{TES}: thermal storage capacity; †: Buck and Giuliano [14]; §: Weiland et al. [19])

$$C = (1 + d{*}T_{reference} + e{*}T_{reference}^2)(a + bx^c)$$

Component	X	Coefficients					Source
		a [USD]	b [USD]	c	d	e	
PHXs	$UA/(W_t/K)$	–	3266.8	0.66	*	*	derived from †
Recuperators	$UA/(W_t/K)$	*	*	*	*	–	
Coolers	$UA/(W_t/K)$	*	*	*	–	–	
ICs	$UA/(W_t/K)$	*	*	*	–	–	
Turbines	P_m/W_m	*	*	*	*	–	
Compressors	$\dot{V}_{in}/(m^3/s)$	*	*	*	–	–	
Motors	P_e/W_e	–	399 400	0.6062	–	–	§
Generator	P_e/W_e	–	108 900	0.5463	–	–	§
Additional piping and valves	sum of costs above	–	5 %	–	–	–	
Piping HP	$\dot{V}_{in}/(m^3/s)$	–	*	*	*	–	
Piping LP	$\dot{V}_{in}/(m^3/s)$	–	*	*	*	–	
Additional sCO_2 BoP	–	2×10^6	–	–	–	–	
Indirect PB cost incl. TP profit	$C_{PB,equipment}$	–	67 %	–	–	–	
Heliostat field	$A_{heliostats}/m^2$	–	110	–	–		†
Receiver	$\dot{Q}_{Rec,t}/kW_t$	–	33	–	–	–	derived from †
1 Tower incl. vertical transport system	H_{tower}/kW_t	560×10^3	913	1.66	–	–	
Horizontal transport system	$\dot{Q}_{Rec,t}/kW_t$	–	6.16	–	–	–	derived from †
Particle inventory	m/kg	–	1.10	–	–	–	†
TES system (excl. inventory)	$Q_{TES}/(kW_th)$	–	6.27	–	–	–	

References

[1] S. Dieckmann, J. Dersch, S. Giuliano, M. Puppe, E. Lüpfert, K. Hennecke, R. Pitz-Paal, M. Taylor, P. Ralon, LCOE reduction potential of parabolic trough and solar tower csp technology until 2025, AIP Conference Proceedings 1850 (2017), https://doi.org/10.1063/1.4984538. URL: https://aip.scitation.org/doi/abs/10.1063/1.4984538.

[2] J. Dyreby, S. Klein, G. Nellis, D. Reindl, Design considerations for supercritical carbon dioxide brayton cycles with recompression, J. Eng. Gas Turbines Power 136 (2014), https://doi.org/10.1115/1.4027936.

[3] Y. Ahn, S.J. Bae, M. Kim, S.K. Cho, S. Baik, J.I. Lee, J.E. Cha, Review of supercritical CO2 power cycle technology and current status of research and development, Nucl. Eng.Technol. 47 (2015) 647–661, https://doi.org/10.1016/j.net.2015.06.009.

[4] F. Crespi, G. Gavagnin, D. Sánchez, G.S. Martínez, Analysis of the thermodynamic potential of supercritical carbon dioxide cycles: a systematic approach, J. Eng. Gas Turbines Power 140 (2017), https://doi.org/10.1115/1.4038125.

[5] S. Glos, M. Wechsung, R. Wagner, A. Heidenhof, D. Schlehuber, Evaluation of sCO2 power cycles for direct and waste heat applications, in: 2nd European sCO2 Conference 2018: 30-31 August 2018, Essen, Germany, 2018, pp. 69–78, doi:10.17185/duepublico/46082.

[6] C.K. Ho, M. Carlson, P. Garg, P. Kumar, Technoeconomic analysis of alternative solarized s-co2 brayton cycle configurations, J. Sol. Energy Eng. 138 (2016), https://doi.org/10.1115/1.4033573.

[7] F. Crespi, D. Sánchez, T. Sánchez, G.S. Martínez, Integral techno-economic analysis of supercritical carbon dioxide cycles for concentrated solar power, in: ASME Turbo Expo 2018: Turbomachinery Technical Conference and Exposition, Volume 9: Oil and Gas Applications; Supercritical CO2 Power Cycles; Wind Energy, 2018, https://doi.org/10.1115/GT2018-77106.

[8] T. Neises, C. Turchi, Supercritical carbon dioxide power cycle design and configuration optimization to minimize levelized cost of energy of molten salt power towers operating at 650 °C, Sol. Energy 181 (2019) 27–36, https://doi.org/10.1016/j.solener.2019.01.078. URL: http://www.sciencedirect.com/science/article/pii/S0038092X19300908.

[9] V.T. Cheang, R.A. Hedderwick, C. McGregor, Benchmarking supercritical carbon dioxide cycles against steam rankine cycles for concentrated solar power, Sol. Energy 113 (2015) 199–211, https://doi.org/10.1016/j.solener.2014.12.016. URL: http://www.sciencedirect.com/science/article/pii/S0038092X14006070.

[10] L. Heller, S. Glos, R. Buck, Sco2 power cycle design without heat source limitations: solar thermal particle technology in the carbosola project, in: 4th European sCO2 Conference for Energy Systems, 2021, https://doi.org/10.17185/duepublico/73961.

[11] W. Wu, L. Amsbeck, R. Buck, R. Uhlig, R. Ritz-Paal, Proof of concept test of a

centrifugal particle receiver, Energy Procedia 49 (2014) 560–568, https://doi.org/10.1016/j.egypro.2014.03.060.
[12] P. Schwarzbözl, R. Pitz-Paal, M. Schmitz, Visual HFLCAL - a software tool for layout and optimisation of heliostat fields, URL: https://elib.dlr.de/60308/, 2009.
[13] M. Ebert, L. Amsbeck, J. Rheinländer, B. Schlögl-Knothe, S. Schmitz, M. Sibum, R. Uhlig, R. Buck, Operational experience of a centrifugal particle receiver prototype, AIP Conference Proceedings 2126 (2019), 030018. URL: https://aip.scitation.org/doi/abs/10.1063/1.5117530. doi:10.1063/1.5117530.
[14] R. Buck, S. Giuliano, Impact of solar tower design parameters on sco2-based solar tower plants, in: 2nd European sCO2 Conference 2018, Conference Proceedings of the European sCO2 Conference, 2018, pp. 160–167, https://doi.org/10.17185/duepublico/46098.
[15] R. Buck, G3P3 techno-economic analysis of UpScaled CentRec® receiver, report, DLR, URL: https://elib.dlr.de/140177/, 2021.
[16] K.J. Albrecht, M.L. Bauer, C.K. Ho, Parametric analysis of particle csp system performance and cost to intrinsic particle properties and operating conditions, in: ASME 2019 13th International Conference on Energy Sustainability Collocated with the ASME 2019 Heat Transfer Summer Conference, 2019, https://doi.org/10.1115/ES2019-3893.
[17] F.M. Crespi, Thermo-economic Assessment of Supercritical CO2 Power Cycles for Concentrated Solar Power Plants, Thesis, University of Seville, 2019.
[18] S. Trevisan, R. Guédez, B. Laumert, Thermo-Economic Optimization of an Air Driven Supercritical CO2 Brayton Power Cycle for Concentrating Solar Power Plant with Packed Bed Thermal Energy Storage, Sol. Energy 211 (2020) 1373–1391, https://doi.org/10.1016/j.solener.2020.10.069. http://www.sciencedirect.com/science/article/pii/S0038092X20311282.
[19] N.T. Weiland, B.W. Lance, S.R. Pidaparti, sCO2 power cycle component cost correlations from DOE data spanning multiple scales and applications, in: ASME Turbo Expo 2019: Turbomachinery Technical Conference and Exposition, Volume Volume 9: Oil and Gas Applications; Supercritical CO2 Power Cycles; Wind Energy, V009T38A008, 2019, https://doi.org/10.1115/gt2019-90493.